

Opposite Structure Learning for Semi-supervised Domain Adaptation

¹Can Qin, ¹Lichen Wang, ²Qianqian Ma, ¹Yu Yin, ¹Huan Wang ^{1,3}Yun Fu

¹ Department of Electrical & Computer Engineering, Northeastern University

²Department of Electrical & Computer Engineering, Boston University

³Khoury College of Computer Science, Northeastern University

qin.ca@husky.neu.edu, wanglichenxj@gmail.com, maqq@bu.edu,
yin.yul@husky.neu.edu, wang.huan@husky.neu.edu, yunfu@ece.neu.edu

Abstract

Current adversarial adaptation methods attempt to align the cross-domain features whereas two challenges remain unsolved: 1) conditional distribution mismatch between different domains and 2) the bias of decision boundary towards the source domain. To solve these challenges, we propose a novel framework for semi-supervised domain adaptation by unifying the learning of opposite structures (UODA). UODA consists of a generator and two classifiers (i.e., the source-based and the target-based classifiers respectively) which are trained with opposite forms of losses for a unified object. The target-based classifier attempts to cluster the target features to improve intra-class density and enlarge inter-class divergence. Meanwhile, the source-based classifier is designed to scatter the source features to enhance the smoothness of decision boundary. Through the alternation of source-feature expansion and target-feature clustering procedures, the target features are well-enclosed within the dilated boundary of the corresponding source features. This strategy effectively makes the cross-domain features precisely aligned. To overcome the model collapse through training, we progressively update the measurement of distance and the feature representation on both domains via an adversarial training paradigm. Extensive experiments on the benchmarks of DomainNet and Office-home datasets demonstrate the effectiveness of our approach over the state-of-the-art method.

1. Introduction

In recent years, Deep Neural Networks (DNNs) are applied to wide-ranging computer vision tasks like image classification, object detection, and semantic segmentation [29, 12, 4, 11] and have proven the superiority in image and video understanding. Despite the great success, DNNs are hungry for vast amounts of labeled data which, however, is

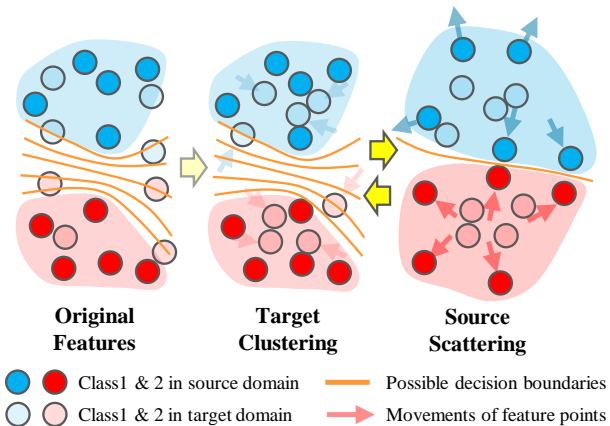


Figure 1. Illustration of the Opposite Structure Learning. During the alternation of **target feature clustering** and **source feature scattering**, the target features are well enclosed within the expanded boundary of corresponding source features to safely align the cross-domain features.

time-consuming and expensive to collect manually.

Domain Adaptation (DA) [22, 5, 2] is proposed to solve this problem by training a model utilizing the labeled data in source domain to make it well-generalized on the label-scarce target domain. The crucial challenge of DA is the shift of distributions (i.e., domain gap) between features of different domains, which violate the distribution-sharing assumption of conventional machine learning algorithms. To mitigate the domain gap, feature alignment methods attempt to project the raw data into a shared feature space to learn domain-invariant features. In this way, the feature divergence or distance are minimized. Based on the measurements of feature divergence, various feature alignment methods, such as Correlation Alignment (CORAL) [30], Maximum Mean Discrepancy (MMD) [16] and Geodesic Flow Kernel (GFK) [9, 8], have been proposed. Currently, adversarial domain alignment methods (i.e., DANN [7], ADDA [33]) have attracted increasing attentions by designing a zero-sum game between a domain classifier and

a feature generator which attempts to fool the discriminator. The features of different domains will be mixed when the discriminator cannot differentiate the source and target features. However, the adversarial adaptation methods are only capable of aligning the marginal distributions of cross-domain features where the conditional distributions remain mismatched due to the scare of labeled target samples.

Recently, it is found that learning well-clustered target features proved to be helpful in conditional distributions alignment. Both DIRT-T [28] and MME [24] applied entropy loss on target features to implicitly group them as multiple clusters in the feature space to keep the discriminative structures through adaptation. In this case, the clustered target features would be aligned with the corresponding source features in a more precise way. However, due to the imbalance of the labeled data between the two domains, the decision boundary is still biased towards the source domain which brings two negative effects: 1) the target features near the boundary might be easily driven to the wrong sides; 2) the boundary would cross the high-density region of target features to mistakenly split them.

According to our observation that the noisy labels is helpful to boost the performance on DA, we further infer that the bias of decision boundary towards the source domain can also be mitigated by learning messy and scattered source features as the regularization. To this end, a good representation for DA would be comprehensively summarised as 1) well-clustered target features for conditional distribution matching and 2) well-scattered source features to regulate the biased model. In this paper, we propose a novel semi-supervised domain adaptation framework with a generator and two classifiers (*i.e.*, the source-based classifier and the target-based classifier) by unifying the learning of these opposite structures (UODA).

In our proposed approach, the target-based classifier clusters the target features in an explicit way via the conditional entropy. While the source-based classifier addresses the bias on source domain by scattering the source features in which the decision boundary becomes more smooth and lays in the middle of the separable class-wise centers. As shown in Fig. 1, through the alternation of source feature expansion and target feature clustering, the target features are well enclosed within the dilated boundary of corresponding source features to makes the conditional distribution of cross-domain features precisely aligned. Moreover, the decision boundary only crosses the low-density region of target features which further enforces the inter-class divergence. To overcome the model collapse through training, we progressively update the measurement of distance and the feature representation on both domains via an adversarial training paradigm. Our proposed model is trained in an end-to-end manner and is friendly for implementation. In summary, the contributions of our framework are below:

- A good representation for DA could be empirically summarised as a contradictory structure including 1) well-clustered target features and 2) well-scattered source features.
- Inspired by the unity of these opposites, we propose a novel semi-supervised domain adaptation framework by unifying the learning of opposite structures (UODA) which both reduce the bias of decision boundary on source domain and align the conditional distribution of cross-domain features.
- Extensive experiments on the benchmarks of DomainNet and Office-home demonstrate the effectiveness of our approach over the state-of-the-art methods.

2. Related Works

Domain Adaptation can be classified as Semi-supervised Domain Adaptation (SSDA) and Unsupervised Domain Adaptation (UDA) with the details below.

2.1. Unsupervised Domain Adaptation (UDA)

The Unsupervised Domain Adaption (UDA), referred as no labels accessible in target domain, is one of the most challenging scenarios in domain adaptation. The generalization of UDA algorithms can be theoretically bounded into three parts: 1) generalization on source domain, 2) the $\mathcal{H}\Delta\mathcal{H}$ -divergence between the source and target features and 3) a constant term [1]. Due to the distribution shift (*i.e.*, domain gap) of the features between different domains, the assumption, training and testing set sharing the same distribution, of conventional machine learning methods are violated. In recent years, many UDA approaches have been proposed [20, 6, 14, 3, 35, 36] to address this problem by learning a mapping function to project the raw images into a shared feature space where the representations of the two domains can be aligned by minimizing the divergence.

Currently, Deep Learning models are widely applied in UDA as the feature extraction function due to their impressive capacity in representation learning. A natural idea of DL-based UDA is to minimize certain kinds of divergence or distance measured by the first-order or second-order statistics between cross-domain deep features. Various methods, such as Deep Maximum Mean Discrepancy (Deep-MMD) [16] or Deep Correlation Alignment (Deep-CORAL) [31] have been proposed. However, the pre-defined distance is weak in measuring the distribution shift of deep features with high dimensions distributed in complicated manifolds. Other popular approaches utilize adversarial training to learn domain invariant representations from a deep generator by fooling a domain classifier (discriminator) with the help of gradient reverse (*i.e.*, GredRev [6]), or GAN-based objectives (*i.e.*, ADDA [33]). CyCADA [13] extends ADDA by introducing a cycleGAN [37] model to

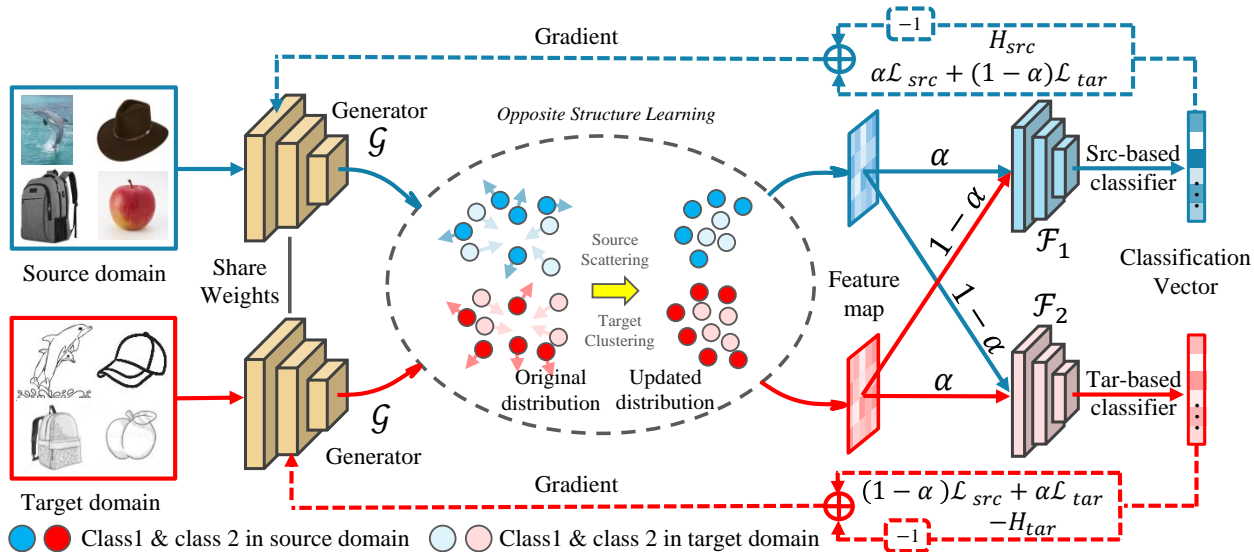


Figure 2. Illustration of the UODA framework which is composed of three parts: 1) a deep feature generator \mathcal{G} ; 2) a source based classifier \mathcal{F}_1 and 3) a target based classifier \mathcal{F}_2 . \oplus denotes element-wise sum. The gradients of entropy losses (i.e., H_{src} and H_{tar}) are reversed when flowing to the generator for adversarial training. Through the opposite structure learning, the clustered target features are well-enclosed by the scattered source features for the safe domain adaptation.

generate pseudo samples with the mix of source domain content and target domain style of for low-level adaption.

Another critical issue is the conditional distributions remain mismatched after adversarial adaption. Tri-training [25] and Co-training [23] applied multiple classifiers to infer the high confident pseudo labels from different views to presumptively denote the conditional distribution of target features. Currently, learning well-clustered target features proved to be helpful in aligning the conditional distributions. DIRT-T [28] applied entropy loss on target features to improve the intra-class density and inter-class divergence to make decision boundaries cross the gap of clustered target features. MCD [27] solves this problem by replacing the discriminator with two classifiers. The decision boundaries learned by the two classifiers provide different support to target features which can be aligned with source features through adversarial training. However, due to the inaccessibility of labeled target samples, UDA methods have limited potentials.

2.2. Semi-supervised Domain Adaptation (SSDA)

In Semi-supervised Domain Adaptation (SSDA), or referred as Few-shot Domain Adaptation (FSDA), the target domain samples are partially labeled. Compared with UDA, collecting limited labeled samples takes little cost, which, however, yields great gains in performance. Therefore, SSDA has attracted the increasing attentions recently.

In SSDA, the conditional distribution of target features can be denoted in a more detailed way due to the accessibility to labeled target samples which makes the cross-

domain features more precisely aligned. Although all the UDA methods can be directly applied to SSDA by adding labeled target samples to the training set, the learnt model would be overfitted to the target set due to the imbalanced training samples.

To solve the problem above, [32] firstly maximizes domain confusion by aligning the marginal distributions of cross-domain features. Then, it applies soft label scores for a matching loss to transfer the semantic relationship from the source domain to the target domain. In CCSA [19], few labeled target samples are utilized to minimize the semantic alignment loss for conditional distribution matching and it simultaneously maximizes the distance between the samples in the same class but from different domains with the help of separation loss. FADA [18] extends CCSA by designing an adversarial training paradigm between a deep generator and multiple binary discriminators to semantically align the cross-domain features and augment the distinguishment between different classes at the same time. MME [24] alternatively updates the estimated class-wise prototypes in the classifier to maximize the entropy on the unlabeled target domain. Furthermore, it clusters features around the estimated prototype by the minimization of entropy with respect to the feature extractor. However, due to the imbalanced labeled data between source and target domains, the decision boundary is still biased towards the source domain. This situation makes the decision boundaries easily cross the density region of target samples or drive the easily confused target features to the wrong side.

3. Our Approach

As shown in Fig. 2, the framework of our model consists of three components: 1) the generator, 2) the source-based classifier, and 3) the target-based classifier. In general, the source-based classifier aims to learn well-scattered source features while the target-based classifier is designed to cluster target features to encourage class-wise alignment. We will analyze each component in details and explain the training procedure in the following parts. Also, we will provide theoretical analysis about the effectiveness of the proposed model.

3.1. Domain Based Classifiers

The goal of SSDA is to build a model that generalizes well on the target domain based on the training set of fully labeled source domain samples and partially labeled target domain samples. To this end, given that we have access to the source images $\mathcal{S} = \{\mathbf{x}_i^s, y_i^s\}_{i=1}^{N_s}$ as well as part of the labeled target images $\mathcal{T} = \{\mathbf{x}_i^t, y_i^t\}_{i=1}^{N_t}$, where $\mathbf{x}_i^s, \mathbf{x}_i^t$ represent the features, y_i^s, y_i^t represent the corresponding labels, $N_s = |\mathcal{S}|, N_t = |\mathcal{T}|$ indicate the number of samples in \mathcal{S} and \mathcal{T} respectively. Moreover, the unlabeled target images set is denoted as $\mathcal{U} = \{\mathbf{x}_i^u\}_{i=1}^{N_u}$, where $N_u = |\mathcal{U}|$. Since such two domains may have different marginal distributions, *i.e.*, $p(\mathbf{x}^s) \neq p(\mathbf{x}^t)$, as well as distinct conditional distributions, *i.e.*, $p(y^s|\mathbf{x}^s) \neq p(y^t|\mathbf{x}^t)$, the model trained only by the labeled samples usually performs poorly on the target domain.

Our proposed method attempts to align the features of the two domains with a feature generator network \mathcal{G} and two classifier networks $\mathcal{F}_1(\cdot)$ and $\mathcal{F}_2(\cdot)$. Compared with the DA methods with only one classifier, the two classifiers which are trained over different losses, learn the decision boundaries from two distinct views so that they are more robust towards the noisy samples [23]. Moreover, this one-generator-two-classifiers structure is also helpful in inferring high confident pseudo labels for the further finetuning of the model. In our approach, the generator $\mathcal{G}(\cdot)$ is utilized to extract the feature $\mathbf{h} \in \mathbb{R}^d$ of any input image \mathbf{x} from the whole training set:

$$\mathbf{h} = \mathcal{G}(\mathbf{x}), \quad (1)$$

where $\mathcal{G}(\cdot)$ is the feature encoder function, which is parameterized by $\Theta_{\mathcal{G}}$. The two classifier networks $\mathcal{F}_1(\cdot)$ and $\mathcal{F}_2(\cdot)$ take the features \mathbf{h} from the generator \mathcal{G} as inputs and classify them into K classes:

$$\begin{aligned} \mathbf{p}_1(y|\mathbf{x}) &= \sigma(\mathcal{F}_1(\mathbf{h}(\mathbf{x}))), \\ \mathbf{p}_2(y|\mathbf{x}) &= \sigma(\mathcal{F}_2(\mathbf{h}(\mathbf{x}))), \end{aligned} \quad (2)$$

where $\mathbf{p}_1(y|\mathbf{x}), \mathbf{p}_2(y|\mathbf{x}) \in \mathbb{R}^K$ denote the K -dimensional probabilistic softmax results of classification functions $\mathcal{F}_1(\cdot)$ and $\mathcal{F}_2(\cdot)$ of the input \mathbf{x} . $\Theta_{\mathcal{F}_1}$ and $\Theta_{\mathcal{F}_2}$ represent the sets of parameters of $\mathcal{F}_1(\cdot)$ and $\mathcal{F}_2(\cdot)$ respectively.

The loss to minimize the empirical risk is composed of two parts: the source domain task loss \mathcal{L}_{src} and the target domain task loss \mathcal{L}_{tar} , which are formulated as follows:

$$\mathcal{L}_{src} = -\mathbb{E}_{(\mathbf{x}^s, y^s) \sim \mathcal{S}} \sum_{k=1}^K \mathbf{1}_{[k=y^s]} \log(p_1(y = y^s|\mathbf{x}^s)), \quad (3)$$

$$\mathcal{L}_{tar} = -\mathbb{E}_{(\mathbf{x}^t, y^t) \sim \mathcal{T}} \sum_{k=1}^K \mathbf{1}_{[k=y^t]} \log(p_2(y = y^t|\mathbf{x}^t)), \quad (4)$$

where $p_1(y = y^s|\mathbf{x}^s), p_2(y = y^t|\mathbf{x}^t)$ represents the k -th dimension of the softmax conditional probability $\mathbf{p}_1(y|\mathbf{x})$ and $\mathbf{p}_2(y|\mathbf{x})$ respectively.

To train the domain based classifiers, as illustrated in Fig 2, we apply asymmetric weights on \mathcal{L}_{src} and \mathcal{L}_{tar} according to a hyper-parameter α where the task loss for $\mathcal{F}_1(\cdot)$ is $\alpha\mathcal{L}_{src} + (1-\alpha)\mathcal{L}_{tar}$, and $(1-\alpha)\mathcal{L}_{src} + \alpha\mathcal{L}_{tar}$ for $\mathcal{F}_2(\cdot)$.

3.2. Unity of Opposite Structure Learning

Apart from learning robust decision boundaries relying on domain based classifiers, we propose the Unity of Opposite Structure Learning for Semi-supervised Domain Adaptation (UODA) which makes the two classifiers learn both well-scattered source features and well-clustered target features in a shared feature space.

In Dirt-T [28] and MME [24], the minimization of conditional entropy on predicted softmax scores proves to be an effective way to cluster the features by enforcing the high confident predictions. In this way, the features would be gathered and drove away from the decision boundary. Followed by these, we apply the conditional entropy loss of unlabeled samples to the target based classifier $\mathcal{F}_2(\cdot)$ to learn the well-clustered features:

$$H_{tar} = -\mathbb{E}_{\mathbf{x}^u \sim \mathcal{U}} \sum_{k=1}^K [p_2(y = k|\mathbf{x}^u) \log p_2(y = k|\mathbf{x}^u)], \quad (5)$$

where $p_2(y = k|\mathbf{x}^u)$ denotes the possibility of data \mathbf{x}^u as the class k which is the k -th dimension of $\mathbf{p}_2(y|\mathbf{x}^u) = \sigma(\mathcal{F}_2(\mathbf{h}(\mathbf{x}^u)))$.

Feature scattering can be regarded as the inverse process of feature clustering. To this end, we will also use conditional entropy loss H_{src} to implement the source feature expansion. The definition of H_{src} is given as follow:

$$H_{src} = -\mathbb{E}_{\mathbf{x}^s \sim \mathcal{S}} \sum_{k=1}^K [p_1(y = k|\mathbf{x}^s) \log p_1(y = k|\mathbf{x}^s)], \quad (6)$$

where $p_1(y = k|\mathbf{x}^s)$ denotes the possibility of the source image \mathbf{x}^s as the class k which is the k -th dimension of $\mathbf{p}_1(y|\mathbf{x}^s) = \sigma(\mathcal{F}_1(\mathbf{h}(\mathbf{x}^s)))$.

3.3. Training Procedure

The training procedure contains the optimization of 3 sets of parameters. $\Theta_{\mathcal{F}_1}$, $\Theta_{\mathcal{F}_2}$ and $\Theta_{\mathcal{G}}$ representing the parameters of the source based classifier $\mathcal{F}_1(\cdot)$, target based classifier $\mathcal{F}_2(\cdot)$ and feature generator $\mathcal{G}(\cdot)$ respectively.

According to the assumption of our method, a good representation for SSDA could be summarized as a seemingly contradictory structure including 1) well-scattered source features and 2) well-clustered target features. To do this, we take the adversarial training on conditional entropy loss followed by MME [24] which progressively updates the class-wise prototypes and the measurement of scarceness in an explicit way. To optimize the domain based classifiers, we firstly apply the asymmetric weights on the task losses to minimize the empirical risk. Then, we maximize the entropy loss of target domain samples on $\mathcal{F}_2(\cdot)$ to update the class-wise prototypes and minimize the entropy loss of source domain samples on $\mathcal{F}_1(\cdot)$ to make source features slightly gathered:

$$\Theta_{\mathcal{F}_1}^* = \arg \min_{\Theta_{\mathcal{F}_1}} \alpha \mathcal{L}_{src} + (1 - \alpha) \mathcal{L}_{tar} + \beta H_{src}, \quad (7)$$

$$\Theta_{\mathcal{F}_2}^* = \arg \min_{\Theta_{\mathcal{F}_2}} (1 - \alpha) \mathcal{L}_{src} + \alpha \mathcal{L}_{tar} - \lambda H_{tar}. \quad (8)$$

where λ and β are hyper-parameters to balance the influence of entropy loss and task loss. The minimization of entropy loss enforces the confidence of classification results by driving the features away from the decision boundary which implicitly makes the features gathered. In turn, maximizing the entropy loss leads to feature scattering.

To progressively cluster the target features and disperse source features, the generator is optimized by the reversal of entropy loss where we minimize the target entropy loss for grouping and maximize the source entropy loss for scattering. The task losses of the two domains are summed for empirical risk minimization:

$$\Theta_{\mathcal{G}}^* = \arg \min_{\Theta_{\mathcal{G}}} \mathcal{L}_{src} + \mathcal{L}_{tar} - \beta H_{src} + \lambda H_{tar}. \quad (9)$$

The whole framework is trained in an end-to-end manner with the help of gradient reversal [7] for adversarial training and stops when reaching certain quantity of epochs.

3.4. Theoretical Insights

We theoretically analyze the effectiveness of our model. Based on the theory in [1], we can bound the risk on the target domain by suming of the risk on source domain and the domain divergence \mathcal{H} -distance, *i.e.*,

$$\forall h \in H, \quad \mathcal{R}_{\mathcal{T}}(h) \leq \mathcal{R}_{\mathcal{S}}(h) + \frac{1}{2} d_{\mathcal{H}}(\mathcal{S}, \mathcal{T}) + \delta, \quad (10)$$

where \mathcal{T} and \mathcal{S} represent the target domain and source domain respectively. $\mathcal{R}_{\mathcal{T}}(h)$ is the expected risk on domain

Algorithm 1 Unity of Opposite Structure Learning for Semi-supervised Domain Adaptation (UODA)

Input:

Labeled source set \mathcal{S} , labeled target set \mathcal{T} and unlabeled target set \mathcal{U} . The number of training epochs T . The randomly initialized parameters $\Theta_{\mathcal{G}}^0$, $\Theta_{\mathcal{F}_1}^0$ and $\Theta_{\mathcal{F}_2}^0$. The hyper-parameters α , β and λ .

Output:

The final parameters $\Theta_{\mathcal{G}}^*$, $\Theta_{\mathcal{F}_1}^*$ and $\Theta_{\mathcal{F}_2}^*$

- 1: $t \leftarrow 0$
 - 2: **while** $t < T$ **do**
 - 3: $t \leftarrow t + 1$.
 - 4: update $\Theta_{\mathcal{F}_1}^{t-1}$ to $\Theta_{\mathcal{F}_1}^t$ by Eq. (7).
 - 5: update $\Theta_{\mathcal{F}_2}^{t-1}$ to $\Theta_{\mathcal{F}_2}^t$ by Eq. (8).
 - 6: update $\Theta_{\mathcal{G}}^{t-1}$ to $\Theta_{\mathcal{G}}^t$ by Eq. (9).
 - 7: **end while**
 - 8: **return** $\Theta_{\mathcal{G}}^* \leftarrow \Theta_{\mathcal{G}}^T$, $\Theta_{\mathcal{F}_1}^* \leftarrow \Theta_{\mathcal{F}_1}^T$ and $\Theta_{\mathcal{F}_2}^* \leftarrow \Theta_{\mathcal{F}_2}^T$.
-

\mathcal{T} . $\mathcal{R}_{\mathcal{S}}(h)$ is the expected risk on domain \mathcal{S} . $d_{\mathcal{H}}(p, q)$ represents the \mathcal{H} -distance of distribution p and q . δ is a constant which is decided by the complexity of the hypothesis space and the error of a perfect hypothesis for both domains. As a consequence, if we train the domain classifiers and the feature extractors with low divergence $d_{\mathcal{H}}(\mathcal{S}, \mathcal{T})$, we can get corresponding low risk on the target domain. Now, we will show how our proposed model is connected to this theory. Since $d_{\mathcal{H}}(\mathcal{S}, \mathcal{T})$ can be written as

$$d_{\mathcal{H}}(\mathcal{S}, \mathcal{T}) = 2 \sup_{h \in \mathcal{H}} \left| \Pr_{\mathbf{f}^s \sim p} [h(\mathbf{f}^s) = 1] - \Pr_{\mathbf{f}^t \sim q} [h(\mathbf{f}^t) = 1] \right|, \quad (11)$$

where \mathbf{f}^s and \mathbf{f}^t represents the features extracted from domain \mathcal{S} and domain \mathcal{T} respectively. In our model, we apply the entropy function $H(\cdot)$ with respect to target domain and source domain to train the parameters of $\mathcal{F}_1(\cdot)$, $\mathcal{F}_2(\cdot)$ and $\mathcal{G}(\cdot)$. Though the entropy function is not the usual classification loss, our model can also be considered as minimizing divergence (11) via adversarial training strategy on domain \mathcal{T} and domain \mathcal{S} respectively. Let h be a binary classifier whose label is decided by the value of the corresponding entropy function:

$$h(\mathbf{f}) = \begin{cases} 1 & \text{if } H(\mathcal{F}_i(\mathbf{f})) \geq \gamma, \\ 0 & \text{otherwise} \end{cases}, \quad (12)$$

where $i = 1, 2$, and γ is a threshold of the classifier. To facilitate analysis, we just assume the output of the classifiers $\mathcal{F}_1(\cdot)$ and $\mathcal{F}_2(\cdot)$ are the conditional probabilities. In

this case, we can obtain

$$\begin{aligned}
 & d_{\mathcal{H}}(\mathcal{S}, \mathcal{T}) \\
 &= 2 \sup_{h \in \mathcal{H}} \left| \Pr_{\mathbf{f}^s \sim p} [h(\mathbf{f}^s) = 1] - \Pr_{\mathbf{f}^t \sim q} [h(\mathbf{f}^t) = 1] \right| \\
 &= 2 \sup_{\mathcal{F}_1, \mathcal{F}_2} \left| \Pr_{\mathbf{f}^s \sim p} [H(\mathcal{F}_1(\mathbf{f}^s)) \geq \gamma] - \Pr_{\mathbf{f}^t \sim q} [H(\mathcal{F}_2(\mathbf{f}^t)) \geq \gamma] \right| \\
 &= 2 \sup_{\mathcal{F}_1, \mathcal{F}_2} \left(\Pr_{\mathbf{f}^t \sim q} [H(\mathcal{F}_2(\mathbf{f}^t)) \geq \gamma] - \Pr_{\mathbf{f}^s \sim p} [H(\mathcal{F}_1(\mathbf{f}^s)) \geq \gamma] \right), \tag{13}
 \end{aligned}$$

where the third equality is due to the assumption that $\Pr_{\mathbf{x}^t \sim q} [H(\mathcal{F}_2(\mathbf{f}^t)) \geq \gamma] \geq \Pr_{\mathbf{x}^s \sim p} [H(\mathcal{F}_1(\mathbf{f}^s)) \geq \gamma]$. This is reasonable since we have access to the label of all the data in the source domain, which means that we can make the corresponding entropy be 0. Replace sup with max in (13), we can rewrite (13) as follows.

$$\begin{aligned}
 & d_{\mathcal{H}}(\mathcal{S}, \mathcal{T}) \\
 &= 2 \max_{\mathcal{F}_1, \mathcal{F}_2} \left(\Pr_{\mathbf{f}^t \sim q} [H(\mathcal{F}_2(\mathbf{f}^t)) \geq \gamma] - \Pr_{\mathbf{f}^s \sim p} [H(\mathcal{F}_1(\mathbf{f}^s)) \geq \gamma] \right) \\
 &= \min_{\mathcal{F}_2} -2 \Pr_{\mathbf{f}^t \sim q} [H(\mathcal{F}_2(\mathbf{f}^t)) \geq \gamma] \tag{14} \\
 &\quad + \min_{\mathcal{F}_1} 2 \Pr_{\mathbf{f}^s \sim p} [H(\mathcal{F}_1(\mathbf{f}^s)) \geq \gamma], \tag{15}
 \end{aligned}$$

which exactly matches with the update rules (7), (8) in our model. Moreover, we aim to minimize the divergence $d_{\mathcal{H}}(\mathcal{S}, \mathcal{T})$ with respect to the features \mathbf{f}^s and \mathbf{f}^t to bound the risk on domain \mathcal{T} , i.e.,

$$\begin{aligned}
 & \min_{\mathbf{f}^s, \mathbf{f}^t} \left\{ \min_{\mathcal{F}_2} -2 \Pr_{\mathbf{f}^t \sim q} [H(\mathcal{F}_2(\mathbf{f}^t)) \geq \gamma] \right. \\
 & \quad \left. + \min_{\mathcal{F}_1} 2 \Pr_{\mathbf{f}^s \sim p} [H(\mathcal{F}_1(\mathbf{f}^s)) \geq \gamma] \right\}, \tag{16}
 \end{aligned}$$

where finding minimum with respect to \mathbf{f}^s and \mathbf{f}^t is equivalent to finding the feature extractor $\mathcal{G}(\cdot)$ to achieve that minimum, which corresponds to the step (9) in our model. Therefore, via iteratively train $\mathcal{F}_1(\cdot)$, $\mathcal{F}_2(\cdot)$ and $\mathcal{G}(\cdot)$, we approximate the optimal solution for problem (16). In other words, we can minimize the divergence $d_{\mathcal{H}}(\mathcal{S}, \mathcal{T})$ to effectively reduce the risk on target domain \mathcal{T} .

4. Experiments

We provide comprehensive evaluations of the proposed method on the semi-supervised domain adaptation (SSDA) and compare with the state-of-the-art approaches. Details of experiments are described in the following sections.

4.1. Experiments Setup

Implementation Details. We deploy the Resnet34 [12] and VGG16 [29] as the backbones of the generator $\mathcal{G}(\cdot)$.

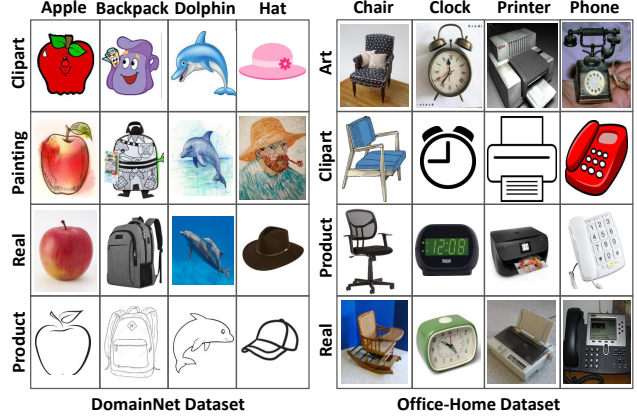


Figure 3. Example images of DomainNet [21] and Office-home [34] Datasets. Compared with the Office-home, DomainNet is a recent dataset involved with more challenging examples.

The two classifiers $\mathcal{F}_1(\cdot)$ and $\mathcal{F}_2(\cdot)$ take a two-layer MLP with randomly initialised weights. To optimize the proposed model, we apply momentum Stochastic Gradient Descent (SGD) as the optimizer implemented on the platform of PyTorch¹. The learning rate is assigned as 0.01 and the momentum is 0.9 with weight decay 0.0005. To balance the influence of different losses on the object function, the hyper-parameters α , β and λ are assigned as 0.75, 0.1, and 0.1 respectively. We regard the unlabeled target samples with the same predictions on both classifiers as the pseudo labeled data which are used for supplements of the training set.

Benchmarks. Our proposed approach and the baseline methods are comprehensively evaluated on the benchmarks of DomainNet² [21] and Office-home³ [34] which are shown in Fig. 3. DomainNet is a multi-source domain adaptation benchmark containing 6 domains and about 600,000 images among 345 categories. For a fair evaluation, we take the same protocol of MME [24] where 4 domains including *Real* (**R**), *Clipart* (**C**), *Painting* (**P**) and *Sketch* (**S**) with 126 classes picked for evaluation. There are 7 adaptation scenarios organized by these 4 domains which yield different scales of domain gap. The Office-home dataset is a well explored UDA benchmark which consists of 4 domains including *Real* (**R**), *Clipart* (**C**), *Art* (**A**) and *Product* (**P**) with 65 classes. We have organized 12 adaptation scenarios in total to evaluate the proposed method.

Evaluation. Given the access to labeled samples in both domains and the unlabeled target domain samples for training, all the models would be evaluated on the unseen samples (*i.e.*, test set) of target domain. We repeat the experiments of our proposed method over three times to report the average top-1 classification accuracy in all tables. All

¹<https://pytorch.org/>

²<http://ai.bu.edu/M3SDA/>

³<http://hemanthdv.org/OfficeHome-Dataset/>

Table 1. Quantitative results (%) on the benchmark of DomainNet.

Methods	R→C		R→P		P→C		C→S		S→P		R→S		P→R		Avg	
	1_{shot}	3_{shot}	1_{shot}	3_{shot}	1_{shot}	3_{shot}	1_{shot}	3_{shot}	1_{shot}	3_{shot}	1_{shot}	3_{shot}	1_{shot}	3_{shot}	1_{shot}	3_{shot}
S+T	55.6	60.0	60.6	62.2	56.8	59.4	50.8	55.0	56.0	59.5	46.3	50.1	71.8	73.9	56.9	60.0
DANN [7]	58.2	59.8	61.4	62.8	56.3	59.6	52.8	55.4	57.4	59.9	52.2	54.9	70.3	72.2	58.4	60.7
ADR [26]	57.1	60.7	61.3	61.9	57.0	60.7	51.0	54.4	56.0	59.9	49.0	51.1	72.0	74.2	57.6	60.4
CDAN [15]	65.0	69.0	64.9	67.3	63.7	68.4	53.1	57.8	63.4	65.3	54.5	59.0	73.2	78.5	62.5	66.5
ENT [10]	65.2	71.0	65.9	69.2	65.4	71.1	54.6	60.0	59.7	62.1	52.1	61.1	75.0	78.6	62.6	67.6
MME [24]	70.0	72.2	67.7	69.7	69.0	71.7	56.3	61.8	64.8	66.8	61.0	61.9	76.1	78.5	66.4	68.9
Ours	72.7	75.4	70.3	71.5	69.8	73.2	60.5	64.1	66.4	69.4	62.7	64.2	77.3	80.8	68.5	71.2

The applied backbone is Resnet34 [12] and Avg means the average results on previous adaptation scenarios.

the methods are evaluated under the one-shot and three-shot settings following [24] where there are one or three labeled samples per class in the target domain.

Baselines. S+T is the approach trained by only the labeled source and target images without adaptation. DANN [7] is an adversarial adaptation method that applies a discriminator to confuse the source and target features with the help of gradient reversal. ADR [26] is a GAN-based method applied to learn both domain-invariant and discriminative features. CDAN [15] is designed for UDA which employs the entropy to control the uncertainty of predictions results to enforce the transferability. ENT [10] is a non-adversarial method which minimizes both the empirical risk on labeled samples and the conditional entropy on unlabeled targets samples. MME [24] is the state-of-the-art SSDA method, the conditional entropy of the unlabeled target samples is minimized by the adversarial training.

4.2. Results on DomainNet

The quantitative results on DomainNet dataset are summarized in Table 1. The Resnet34 is deployed as the backbone of the generator. It is easily observed that the proposed method outperforms all the baseline methods on all adaptation scenarios with a large margin. Although the largest domain gap appears on the adaptation scenario *Real to Sketch* (i.e., $R \rightarrow S$). Ours exhibits its superiority in aligning the features of different domains. On the easiest adaptation scenario *Painting to Real* (i.e., $P \rightarrow R$), the accuracy of ours on 3-shot is over 80% which indicates its great potential to put into practice. In comparison to the performance of the both tasks, the improvements on the 1-shot SSDA is slightly inferior to those of the 3-shot which could be explained that more labeled target examples, which is helpful to indicate the target domain conditional distribution, contribute a lot to the semantic feature alignment.

4.3. Results on Office-Home

The quantitative results and comparison on the benchmark Office-home are summarized in Table 2 in which we take VGG16 as the backbone. The baseline methods are outperformed by our proposed method on most of adaptation scenarios which comprehensively demonstrates the su-

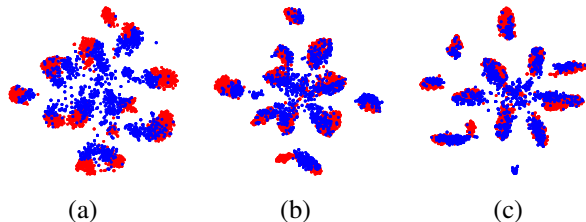


Figure 4. The visualization results of t-SNE [17] on the shared ten-class features on the adaptation scenario *Real to Sketch*, i.e., $R \rightarrow S$, obtained by (a) S+T, (b) MME [24] and (c) Ours. The figures are captured under 3-shot SSDA setting. The feature points of source and target domains are indicated by red and blue spots.

riority of our proposed method, especially on the task of three-shot SSDA. However, on the most challenging adaptation scenarios *Painting to Clipart* (i.e., $P \rightarrow C$) and *Art to Clipart* (i.e., $A \rightarrow C$) under the setting of one-shot SSDA, ours is slightly defeated by the MME. It indicates that the maximization of source entropy has the chance to introduced the negative transfer to feature alignment. This phenomenon might be explained as the scattering of source features can drive the noisy target features to the wrong side if there are no strong constraints like more labeled target samples or other kinds of prior knowledge to regulate. In this way, we further conclude that a limited number of labeled target samples are necessary for our approach.

4.4. Analysis

Ablation Study. To investigate the effects of each module, we introduce the ablation study on the adaptation scenarios *Real to Sketch* (i.e., $R \rightarrow S$) and *Real to Clipart* (i.e., $R \rightarrow C$). As shown in Table 3, we have analyzed five different components including single classifier (i.e., $1-C$) which is of same architecture as MME, two classifiers (i.e., $2-C$) including the source-based and target-based classifiers that applied in our proposed method, target entropy loss (i.e., H_{tar}), both source entropy and target entropy (i.e., $H_{tar}+H_{src}$), and the self-training [23] (i.e., ST) which takes the pseudo labels inferred from the two classifiers to further finetune the model. From the table, we find that the performance has dropped after adding the source entropy loss to $1-C$ which means that one classifier is not good

Table 2. Quantitative results (%) on the benchmark of Office-home.

ONE-SHOT													
Methods	R→C	R→P	R→A	P→R	P→C	P→A	A→P	A→C	A→R	C→R	C→A	C→P	Avg
S+T	39.5	75.3	61.2	71.6	37.0	52.0	63.6	37.5	69.5	64.5	51.4	65.9	57.4
DANN [7]	52.0	75.7	62.7	72.7	45.9	51.3	64.3	44.4	68.9	64.2	52.3	65.3	60.0
ADR [26]	39.7	76.2	60.2	71.8	37.2	51.4	63.9	39.0	68.7	64.8	50.0	65.2	57.4
CDAN [15]	43.3	75.7	60.9	69.6	37.4	44.5	67.7	39.8	64.8	58.7	41.6	66.2	55.8
ENT [10]	23.7	77.5	64.0	74.6	21.3	44.6	66.0	22.4	70.6	62.1	25.1	67.7	51.6
MME [24]	49.1	78.7	65.1	74.4	46.2	56.0	68.6	45.8	72.2	68.0	57.5	71.3	62.7
Ours	49.6	79.8	66.1	75.4	45.5	58.8	72.5	43.3	73.3	70.5	59.3	72.1	63.9

THREE-SHOT													
Methods	R→C	R→P	R→A	P→R	P→C	P→A	A→P	A→C	A→R	C→R	C→A	C→P	Avg
S+T	49.6	78.6	63.6	72.7	47.2	55.9	69.4	47.5	73.4	69.7	56.2	70.4	62.9
DANN [7]	56.1	77.9	63.7	73.6	52.4	56.3	69.5	50.0	72.3	68.7	56.4	69.8	63.9
ADR [26]	49.0	78.1	62.8	73.6	47.8	55.8	69.9	49.3	73.3	69.3	56.3	71.4	63.0
CDAN [15]	50.2	80.9	62.1	70.8	45.1	50.3	74.7	46.0	71.4	65.9	52.9	71.2	61.8
ENT [10]	48.3	81.6	65.5	76.6	46.8	56.9	73.0	44.8	75.3	72.9	59.1	77.0	64.8
MME [24]	56.9	82.9	65.7	76.7	53.6	59.2	75.7	54.9	75.3	72.9	61.1	76.3	67.6
Ours	57.6	83.6	67.5	77.7	54.9	61.0	77.7	55.4	76.7	73.8	61.9	78.4	68.9

The applied backbone is VGG16 [29] and Avg means the average results on previous adaptation scenarios.

Table 3. Quantitative results (%) of ablation study.

COMPONENTS					R→S	R→C
1-C	2-C	\mathcal{H}_{tar}	$\mathcal{H}_{tar}+\mathcal{H}_{src}$	ST	$1_{shot}/\beta_{shot}$	$1_{shot}/\beta_{shot}$
✓		✓			61.0/61.9	70.0/72.2
✓			✓		60.4/61.2	69.2/71.5
	✓	✓			61.1/62.8	70.5/72.4
	✓		✓		62.2/63.9	71.6/74.0
	✓	✓		✓	61.2/62.6	70.7/72.8
	✓		✓	✓	62.7/64.2	72.7/75.4

The applied backbone is Resnet34 [12].

at learning the opposite structures of the two domain features. However, introducing two classifiers **2-C** to optimize the source and target entropy losses has significantly improved the performance. These two phenomenons have sufficiently justified the necessities of the two-classifiers structure for the opposite structures learning. The performance of the proposed method can be improved further by applying self-training to finetune the model. Even without the self-training, ours still outperforms the baseline methods in a large margin.

Convergence Analysis. We evaluate the convergence of baseline methods as well as our proposed methods on the adaptation scenario *Real to Sketch* (i.e., **R→S**) in Fig. 5 (a). It is easily observed that the proposed method would reach the highest score around the 5,000-th epoch and keep stable with little disturbance since that.

Sensitivity of labeled samples. As shown in Fig. 5 (b), we conduct the experiments adapted from the *Real to Sketch* on the settings of 1-shot, 3-shot and 5-shot SSDA. We notice that our proposed method continuously maintains the lead over the baseline methods under all the settings.

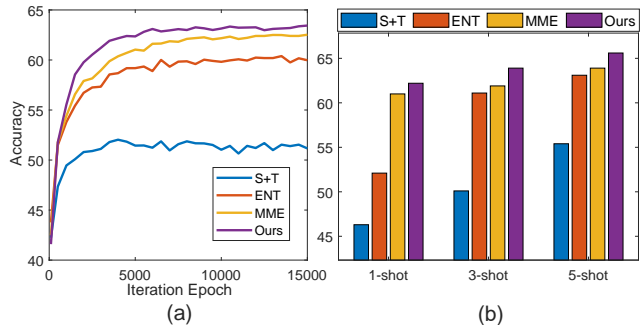


Figure 5. (a) Convergence analysis on *Real to Sketch*. (b) Performance of UODA and other baseline methods under three different settings (i.e., 1-shot, 3-shot and 5-shot) on *Real to Sketch*.

Feature Visualization. In order to better understand the distribution of features, we employ the visualization technique to analyze generator features using t-SNE algorithm [17] which are shown in Fig. 4. Compared with S+T and MME, the features learned by our approach is more clustered and separable where the groups of cross-domain features are more precisely aligned.

5. Conclusion

In this paper, we propose a novel semi-supervised domain adaptation framework (UODA) inspired by the Unity of Opposites. UODA is consisting of a generator and two classifiers (i.e., the source-based classifier and the target-based classifier) designed with the opposite forms of losses for a shared object. The source-based classifier is applied to disperse the source features to regulate the decision boundary less complicated. While the other target-based classifier

is employed to cluster the target features to improve intra-class similarity and inter-class divergence. Through the cooperation of source-feature expansion and target-feature clustering, the target features would be enclosed by the expanded source features which makes the cross-domain features precisely aligned. To overcome the model degradation during training, we apply the adversarial training to progressively update the measurement of feature divergence and its representation on both domains. Extensive experiments on DomainNet and Office-home datasets demonstrate the superiority of our approach over the state-of-the-art ones.

References

- [1] Shai Ben-David, John Blitzer, Koby Crammer, Alex Kulesza, Fernando Pereira, and Jennifer Wortman Vaughan. A theory of learning from different domains. *Machine learning*, 79(1-2):151–175, 2010.
- [2] Bharath Bhushan Damodaran, Benjamin Kellenberger, Rémi Flamary, Devis Tuia, and Nicolas Courty. Deepjdot: Deep joint distribution optimal transport for unsupervised domain adaptation. In *Proceedings of European Conference on Computer Vision*, pages 447–463, 2018.
- [3] Yue Cao, Mingsheng Long, and Jianmin Wang. Unsupervised domain adaptation with distribution matching machines. In *Proceedings of AAAI Conference on Artificial Intelligence*, 2018.
- [4] Marius Cordts, Mohamed Omran, Sebastian Ramos, Timo Rehfeld, Markus Enzweiler, Rodrigo Benenson, Uwe Franke, Stefan Roth, and Bernt Schiele. The cityscapes dataset for semantic urban scene understanding. In *Proceedings of IEEE Conference on Computer Vision and Pattern Recognition*, 2016.
- [5] Zhengming Ding, Sheng Li, Ming Shao, and Yun Fu. Graph adaptive knowledge transfer for unsupervised domain adaptation. In *Proceedings of European Conference on Computer Vision*, pages 37–52, 2018.
- [6] Yaroslav Ganin and Victor Lempitsky. Unsupervised domain adaptation by backpropagation. *arXiv preprint arXiv:1409.7495*, 2014.
- [7] Yaroslav Ganin, Evgeniya Ustinova, Hana Ajakan, Pascal Germain, Hugo Larochelle, François Laviolette, Mario Marchand, and Victor Lempitsky. Domain-adversarial training of neural networks. *The Journal of Machine Learning Research*, 17(1):2096–2030, 2016.
- [8] Boqing Gong, Yuan Shi, Fei Sha, and Kristen Grauman. Geodesic flow kernel for unsupervised domain adaptation. In *Proceedings of IEEE Conference on Computer Vision and Pattern Recognition*, pages 2066–2073, 2012.
- [9] Raghuraman Gopalan, Ruonan Li, and Rama Chellappa. Domain adaptation for object recognition: An unsupervised approach. In *Proceedings of IEEE International Conference on Computer Vision*, pages 999–1006, 2011.
- [10] Yves Grandvalet and Yoshua Bengio. Semi-supervised learning by entropy minimization. In *Advances in neural information processing systems*, pages 529–536, 2005.
- [11] Kaiming He, Georgia Gkioxari, Piotr Dollár, and Ross Girshick. Mask r-cnn. In *Proceedings of IEEE International Conference on Computer Vision*, pages 2961–2969, 2017.
- [12] Kaiming He, Xiangyu Zhang, Shaoqing Ren, and Jian Sun. Deep residual learning for image recognition. In *Proceedings of IEEE Conference on Computer Vision and Pattern Recognition*, 2016.
- [13] Judy Hoffman, Eric Tzeng, Taesung Park, Jun-Yan Zhu, Phillip Isola, Kate Saenko, Alexei A Efros, and Trevor Darrell. Cycada: Cycle-consistent adversarial domain adaptation. *arXiv preprint arXiv:1711.03213*, 2017.
- [14] Mohammad Nazmul Alam Khan and Douglas R Heisterkamp. Adapting instance weights for unsupervised domain adaptation using quadratic mutual information and subspace learning. In *Proceedings of IEEE Conference on International Conference on Pattern Recognition*, 2016.
- [15] Mingsheng Long, Zhangjie Cao, Jianmin Wang, and Michael I Jordan. Conditional adversarial domain adaptation. In *Advances in Neural Information Processing Systems*, pages 1640–1650, 2018.
- [16] Mingsheng Long, Jianmin Wang, Guiguang Ding, Jianguang Sun, and Philip S Yu. Transfer feature learning with joint distribution adaptation. In *Proceedings of IEEE International Conference on Computer Vision*, 2013.
- [17] Laurens van der Maaten and Geoffrey Hinton. Visualizing data using t-sne. *Journal of Machine Learning Research*, 9:2579–2605, 2008.
- [18] Saeid Motiian, Quinn Jones, Seyed Iranmanesh, and Gianfranco Doretto. Few-shot adversarial domain adaptation. In *Advances in Neural Information Processing Systems*, pages 6670–6680, 2017.
- [19] Saeid Motiian, Marco Piccirilli, Donald A Adjeroh, and Gianfranco Doretto. Unified deep supervised domain adaptation and generalization. In *Proceedings of the IEEE International Conference on Computer Vision*, pages 5715–5725, 2017.
- [20] Sinno Jialin Pan, Ivor W Tsang, James T Kwok, and Qiang Yang. Domain adaptation via transfer component analysis. *IEEE Transactions on Neural Networks*, 22(2):199–210, 2011.
- [21] Xingchao Peng, Qinxun Bai, Xide Xia, Zijun Huang, Kate Saenko, and Bo Wang. Moment matching for multi-source domain adaptation. In *Proceedings of the IEEE International Conference on Computer Vision*, pages 1406–1415, 2019.
- [22] Xingchao Peng, Ben Usman, Neela Kaushik, Judy Hoffman, Dequan Wang, and Kate Saenko. Visda: The visual domain adaptation challenge. *arXiv preprint arXiv:1710.06924*, 2017.
- [23] Can Qin, Lichen Wang, Yulun Zhang, and Yun Fu. Generatively inferential co-training for unsupervised domain adaptation. In *Proceedings of the IEEE International Conference on Computer Vision Workshops*, pages 0–0, 2019.
- [24] Kuniaki Saito, Donghyun Kim, Stan Sclaroff, Trevor Darrell, and Kate Saenko. Semi-supervised domain adaptation via minimax entropy. *arXiv preprint arXiv:1904.06487*, 2019.
- [25] Kuniaki Saito, Yoshitaka Ushiku, and Tatsuya Harada. Asymmetric tri-training for unsupervised domain adaptation.

- In *Proceedings of the International Conference on Machine Learning*, pages 2988–2997, 2017.
- [26] Kuniaki Saito, Yoshitaka Ushiku, Tatsuya Harada, and Kate Saenko. Adversarial dropout regularization. *arXiv preprint arXiv:1711.01575*, 2017.
 - [27] Kuniaki Saito, Kohei Watanabe, Yoshitaka Ushiku, and Tatsuya Harada. Maximum classifier discrepancy for unsupervised domain adaptation. In *Proceedings of IEEE Conference on Computer Vision and Pattern Recognition*, pages 3723–3732, 2018.
 - [28] Rui Shu, Hung H Bui, Hirokazu Narui, and Stefano Ermon. A dirt-t approach to unsupervised domain adaptation. *arXiv preprint arXiv:1802.08735*, 2018.
 - [29] Karen Simonyan and Andrew Zisserman. Very deep convolutional networks for large-scale image recognition. *arXiv preprint arXiv:1409.1556*, 2014.
 - [30] Baochen Sun and Kate Saenko. Subspace distribution alignment for unsupervised domain adaptation. In *British Machine Vision Conference*, volume 4, pages 24–1, 2015.
 - [31] Baochen Sun and Kate Saenko. Deep coral: Correlation alignment for deep domain adaptation. In *Proceedings of European Conference on Computer Vision*, 2016.
 - [32] Eric Tzeng, Judy Hoffman, Trevor Darrell, and Kate Saenko. Simultaneous deep transfer across domains and tasks. In *Proceedings of the IEEE International Conference on Computer Vision*, pages 4068–4076, 2015.
 - [33] Eric Tzeng, Judy Hoffman, Kate Saenko, and Trevor Darrell. Adversarial discriminative domain adaptation. In *Proceedings of IEEE conference on Computer Vision and Pattern Recognition*, 2017.
 - [34] Hemanth Venkateswara, Jose Eusebio, Shayok Chakraborty, and Sethuraman Panchanathan. Deep hashing network for unsupervised domain adaptation. In *Proceedings of the IEEE Conference on Computer Vision and Pattern Recognition*, pages 5018–5027, 2017.
 - [35] Jindong Wang, Wenjie Feng, Yiqiang Chen, Han Yu, Meiyu Huang, and Philip S Yu. Visual domain adaptation with manifold embedded distribution alignment. In *Proceedings of ACM Multimedia Conference on Multimedia Conference*, pages 402–410, 2018.
 - [36] Lichen Wang, Zhengming Ding, and Yun Fu. Low-rank transfer human motion segmentation. *IEEE Transactions on Image Processing*, 28(2):1023–1034, 2019.
 - [37] Jun-Yan Zhu, Taesung Park, Phillip Isola, and Alexei A Efros. Unpaired image-to-image translation using cycle-consistent adversarial networks. In *Proceedings of IEEE International Conference on Computer Vision*, 2017.